Plykin type attractor in electronic device simulated in Multisim

Sergey P. Kuznetsov*

An electronic device is suggested representing a non-autonomous dynamical system with hyperbolic chaotic attractor of Plykin type in the stroboscopic map, and the results of its simulation with software packet NI Multisim are considered in comparison with numerical integration of the underlying differential equations. A main practical advantage of electronic devices of this kind is their structural stability that means insensitivity of the chaotic dynamics in respect to variations of functions and parameters of elements constituting the system as well as to interferences and noises.

PACS numbers: 05.45.-a Nonlinear dynamics and nonlinear dynamical systems; 05.45.Ac Low-dimensional chaos; 05.45.Pq Numerical simulations of chaotic systems; 84.30.-r Electronic circuits

Classic Plykin attractor is a limit set for an artificially constructed map defined on a plane or on a sphere characterized by subtle and delicate topological structure. Till now, no examples of such attractors in physical systems were presented, although properties of the associated uniformly hyperbolic chaotic dynamics look appealing for applications due to the intrinsic structural stability (insensitivity of the generated chaos to variation of functions and parameters in governing equations). In this paper an electronic scheme is proposed that gives rise to the attractor of Plykin type in the stroboscopic map, which describes evolution of the states over characteristic time period in the course of operation of the device. Results of simulation with the software product Multisim are considered in comparison with numerical integration of the underlying differential equations.

I. INTRODUCTION

In a frame of possible applications of chaos, like secure communication, cryptography, generating random numbers, it would be highly desirable to deal with systems, in which strong chaotic dynamics is insensitive in respect to variation of functions and parameters in the governing equations. This is the property of roughness, or structural stability. Unfortunately, it is not intrinsic to majority of common chaotic systems.

The concept of roughness was introduced in 1937 by Andronov and Pontryagin and gave rise to a powerful research program in the oscillation theory [1–3]. The rough systems are regarded as those subjected to priority consideration in theory and as the most important for practice. The mentioned research program was developed successfully for flow systems with two-dimensional phase space; however, its generalization for multidimensional dynamics met serious problems and was found to be not achievable, at least in straightforward way. In modern theory of dynamical systems the class of structurally stable systems is distinguished as those satisfying Smale's axiom A and the strong transversality condition [4–12]. Structurally stable are the Morse-Smale systems, which manifest only simple regular dynamics, and systems with uniformly hyperbolic chaotic attractors demonstrating the structurally stable chaos. Just this last type of the dynamical behavior is of interest for us here.

The uniformly hyperbolic attractors were introduced about 40 years ago [2–12], and chaotic nature of the dynamics associated with such attractors is rigorously proven. Initially, it was expected that these attractors will relate to many physical situations, where chaos occurs. However, as the studies and understanding developed, it became clear that concrete attractors arising in the context of applications usually do not fit the narrow frame of the early hyperbolic theory. (E.g., it relates to Lorenz equations, Rössler models, maps of Hénon and Ikeda, electronic generators of chaos, etc.) As to the uniformly hyperbolic attractors, their examples were restricted to artificial mathematical constructions, such as the Smale-Williams solenoid [4, 5] and the Plykin attractor [6].

To be concrete, construction of one version of Plykin type attractor [8, 9] looks as follows. Consider an area depicted in the left part of Figure 1 with three cutouts. A map is defined in such way that the effect on points of this area produces the figure shown to the right. Attractor is the limit set arising under multiple repetition of the mapping. Note that the area under consideration is covered by hatching, indicating two attributed direction fields. After applying the map they remain unchanged that provides the hyperbolic nature of the attractor. In mathematical terminology they are called the foliations. One is referred to as the contracting foliation as associated with contraction and the other is the expanding foliation.

Construction of physical systems manifesting attrac-

*Kotel'nikov's Institute of Radio-Engineering and Electronics of RAS, Saratov Branch, Zelenaya 38, Saratov, 410019, Russian Federation;
Potsdam University, Department of Physics, Karl-Liebknecht-Str. 24/25, 14476 Potsdam-Golm, Germany.

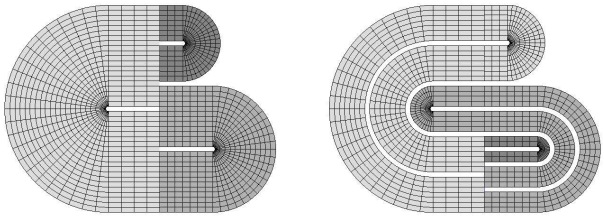

FIG. 1: Construction of the mathematical example of attractor of Plykin type: the initial domain on the plane (left) and the result of its transformation under a single application of the map (right).

tors of this kind seems a challenging problem, as the structure looks complicated, subtle and non-trivial. Until now, there were no concrete examples presented, although it was argued in literature in favor of possible occurrence of Plykin type attractors in Poincaré maps of a modified geometric Lorenz model [13] and of a three-dimensional set of differential equations of the model neuron [14]. Hunt in his thesis suggested an artificial example of a non-autonomous flow system with Plykin-type attractor in the stroboscopic two-dimensional map [15, 16]. His construction, however, is very cumbersome, and it is highly questionable to reproduce it as a real physical device.

Note that recently physically realizable systems were proposed with attractors of Smale-Williams type [17–22]. So, there is a background now for constructing actual operating devices with uniformly hyperbolic attractors that show structurally stable chaos. In particular, it may be electronic circuits, which will have advantages for possible applications because of insensitivity of chaotic dynamics in respect to variation of functions and parameters of elements constituting the system.

Bearing in mind the development of electronic devices, it is natural to turn to computer circuit simulation tools; among them a convenient and popular software product is Multisim [23]. Its original version called the Electronic Workbench was released in 1995 by Interactive Image Technologies Company. Since 2005, improved versions of the software are being developed by National Instruments under the name of NI Multisim. The results presented in the present paper were obtained with the use of the licensed version of NI Multisim 10.1.1 purchased by Saratov Branch of IRE RAS.

This paper presents the scheme and results of simulation in the Multisim for a non-autonomous system of such kind that attractor in the stroboscopic map is just the Plykin type attractor. The idea of constructing the underlying differential equations is based on the previous studies of the author [24–26], although there are some specific features introduced to simplify the schematic implementation.

II. BASIC EQUATIONS AND SOME NUMERICAL RESULTS

It is known that the attractor of Plykin type may be considered as placed on a sphere instead of the plane. A passage from one representation to another corresponds to a change of variables associated with stereographic projection familiar from the elementary geometry.

Consider a sphere of unit radius in a space of three variables x, y, z, which satisfies the equation $x^2+y^2+z^2=1$ (Fig. 2). According to the Plykin result, occurrence of a hyperbolic attractor on a sphere requires presence of at least four holes, the areas not belonging to the attractor. In our construction this will be neighborhoods of four points A, B, C, D with coordinates $(x, y, z) = (\pm 1/\sqrt{2},\ 0,\ \pm 1/\sqrt{2})$.

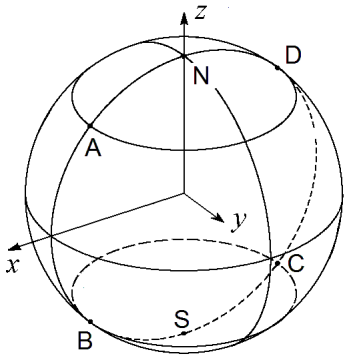

FIG. 2: The unit sphere used in the construction of the basic equations.

First, we introduce the flow along circles of latitude of some time duration T that corresponds to motions of representative points on the sphere away from the meridians containing the arcs AB and CD towards the meridians equally distant from these arcs. It is described by the relations $\dot{x} \sim -xy^2$, $\dot{y} \sim x^2y$ while z remains constant. (It is a kind of dissipative motion on the sphere.) Then, on the final part of the time interval we apply differential rotation of relatively small duration τ around z-axis. The angular velocity is assumed to depend on z linearly in such way that the rotation makes the points launched from A and D to exchange their positions, while the points at B and C remain in the rest. Accounting both superimposed components of the motion, we get the differential equations

$$\begin{aligned} \dot{x} &= K[-\varepsilon xy^2 + \xi(t)(z+D)y], \\ \dot{y} &= K[\varepsilon x^2 y - \xi(t)(z+D)x], \\ \dot{z} &= 0, \end{aligned} \qquad (1)$$

where $\xi(t) = 0$ at $t < T-\tau$, and $\xi(t) = 1$ at $T-\tau \le t < T$. The parameters are supposed to satisfy the conditions $K\tau = \pi/\sqrt{2}$ and $D = 1/\sqrt{2}$, at least approximately. In the next time interval of duration T we assume that analogous motions on the sphere take place, but with exchange of the roles for the axes x and z. The postulated

stages of pair-wise evolution of the variables (x, y) and (y, z) are repeated periodically turn by turn. Intuitively, it looks reasonable that the imposed transformations will generate a flow on the sphere accompanying with formation of filaments of fine transversal structure that is a characteristic feature of the Plykin type attractors.

To finish the formulation, we compliment the equation for y by a term with constant coefficient γ that facilitates approach of orbits in the phase space to the unit sphere, and write down the following set of equations.

$$\begin{aligned}
&\textbf{First half} - \textbf{period}\ [2nT \le t < (2n+1)T]:\\
&\dot{x} = K\left[-\varepsilon xy + \xi(t)\,(z+D)\right] y,\\
&\dot{y} = K\left[\varepsilon xy - \xi(t)\,(z+D)\right] x + \gamma y(1-x^2-y^2-z^2),\\
&\dot{z} = 0.\\
&\textbf{Second half} - \textbf{period}\ [(2n+1)T \le t < 2(n+1)T]:\\
&\dot{x} = 0,\\
&\dot{y} = K\left[\varepsilon yz - \xi(t)\,(x+D)\right] z + \gamma y(1-x^2-y^2-z^2),\\
&\dot{z} = K\left[-\varepsilon yz + \xi(t)\,(x+D)\right] y.
\end{aligned} \tag{2}$$

Here $\xi(t) = 0$ at $t < T - \tau$, $\xi(t) = 1$ at $T - \tau \le t < T$, and $\xi(t+T) = \xi(t)$.

Figure 3 shows phase portraits of the attractor in the stroboscopic section at $t_n = nT$ in projections on the planes (x, y), (x, z), and (z, y) obtained from numerical integration of the equations. The parameter values are

$$K = 1.1,\ \varepsilon = 0.1,\ T = 10,\ \tau = 2,\ \gamma = 0.25. \tag{3}$$

Observe specific fractal-like transverse structure of the attractor: the object looks like composed of strips, each of which contains narrower strips of the next level etc. (Actually, this attractor appears to be topologically equivalent to the construction explained with Figure 1; this matter will be specially discussed in Section IV.)

III. SCHEME OF THE ANALOG DEVICE AND SIMULATION IN MULTISIM

In the design of electronic systems one can use two approaches, although the border between them is evidently a matter of convention [27–29]. One is constructing systems with dynamic behavior qualitatively corresponding to the required one on a base of simple electronic components, like capacitors, inductors, resistors, transistors, voltage sources, feedback elements, etc. The second consists in accurate reproduction of the original equations using blocks elaborated in analog modeling technology, like integrators, multipliers, adders, etc. Basically, the both approaches are appropriate to build real operating electronic devices that act as generators of the structurally stable chaos. However, given the fact that identification of the Plykin attractor is a non-trivial problem, in the present study we deliberately prefer to be closer to the second approach. Then, the argumentation concerning the nature of the attractor may appeal to numerical results relating to the underlying differential equations.

The circuit diagram of the proposed device is shown in Figure 4. The dynamical variables x, y, z correspond to the voltages on the capacitors C3, C2 and C1. The integrator built on the operational amplifier U1 is responsible for the dynamics of z or x, depending on a state of the switches J1 and J2, and the integrator on the amplifier U2 corresponds to the dynamics of y. By means of the multipliers A1, A2, A3 and A6, and with supplied DC voltage from the source V1 through resistor R17, variation of y is managed in such way that the sum of squares of all variables in the course of the dynamical evolution tends to 1. This allows us to interpret the dynamics on the attractor as occurring on the unit sphere in the phase space.

In the course of operation of the scheme two switches J1 and J2 are opened and closed alternately, so that on successive half-periods the dynamical process involves one or another pair of the variables, either (x, y) or (z, y), while the rest variable, z or x, remains nearly constant as the voltage on an open capacitor (C1 or C3). Through the operational amplifier U4 this voltage is applied to the multipliers A5 and A7 controlling the oscillation frequency for the pair of other variables. This is arranged in such way that the frequency depends on the voltage linearly with added constant, determined by the DC source V1. All this takes place in the case of ON state for the switch J3 for some time at the end of each half-cycle of switching for J1 and J2. Dissipative nature of the dynamics on the sphere is provided by signals from the multiplier A4 through the inverting amplifier U5.

The dynamics of the device is described by equations (2), where a unit of time is accepted equal to $\tau_0 = R_0C_0 = 0.1$ ms. (This is a product of the capacitance used in the integrators, C1=C2=C3=C_0=100 nF, and the characteristic impedance R_0=1 kΩ.) Note that the states ON and OFF for the keys J1 and J2 occupy the time intervals of 10 units, i.e. T=1 ms. Also this quantity T is a period of opening and closing for the key J3. The time interval, when it is ON, is the final part of duration 0.2 ms of each period. Parameter K in the equations can be adjusted by simultaneous variation of resistances R14 and R15. Parameter ε is controlled by the resistor R9, parameter D by the resistor R18, and parameter γ by the resistor R4. All these parameters depend on the resistances in inverse proportion. With the nominated parameters in the circuit diagram the values of K, ε, D and γ correspond to those adopted in computations discussed in the previous section.

Figure 5 shows samples of time dependences for three variables obtained from simulation in Multisim using the Four Channel Oscilloscope tool with three inputs linked to the appropriate nodes in the circuit diagram indicated by the letters x, y, and z.

Figure 6 illustrates spectra of the signals generated in the course of operation of the scheme. These pictures are obtained using the Spectrum Analyzer tool in the Multisim with appropriate installation of the working frequency range and resolution of the analysis. The spectra

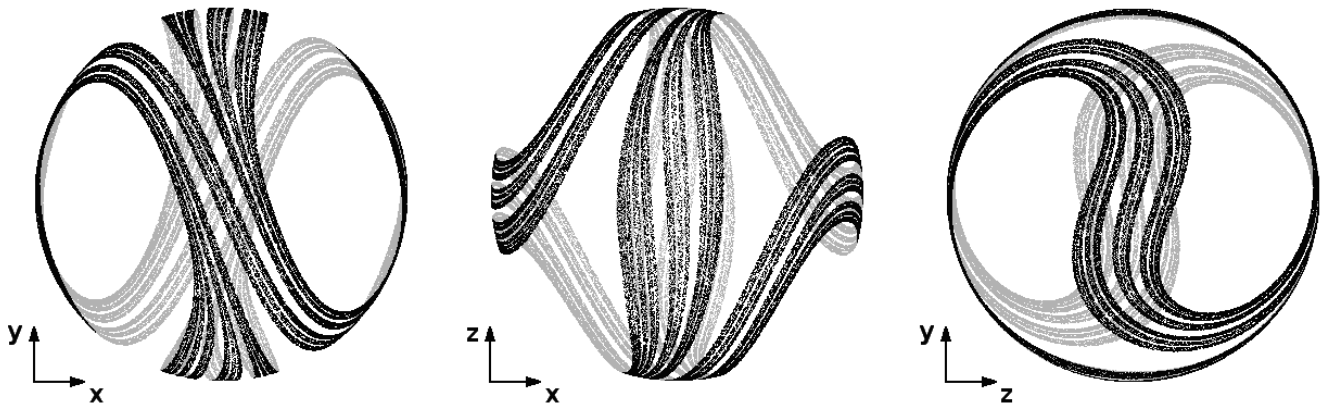

FIG. 3: Stroboscopic portraits of the attractor in three projections obtained from the numerical integration of equations (2). Parameters are assigned according (3)

in Figure 6 are given in linear scale. Upper, middle and bottom panels correspond to the signals x, y and z. Continuous nature of the spectra indicates chaotic dynamics on the attractor. It may be noted that the first and third spectra are visually identical (up to statistical errors), while the spectrum for y looks quite different and shows two pronounced maxima at 200 and 500 Hz. This observation is not surprising because of the symmetrical involvement of the variables x and z in the dynamics of the system.

To observe the attractor in projection on the planes (x, y) (x, z), and (z, y) we connect two input terminals of the Oscilloscope in Multisim to the corresponding nodes of the scheme, and enter the instrument in a mode where the horizontal and vertical deviation of the beam is controlled by input voltages. The obtained portraits are shown in Figure 7. To see correspondence of the simulation results with pictures in Fig. 3 it is necessary to depict the stroboscopic sections of the attractor. Using the same connection of the multi-channel oscilloscope, as that in the analysis of time dependences, we carry out the simulation for a sufficiently long interval, say, 10^5 periods of switching. Then, the Grapher tool in Multisim is used, which supports record of data in a file, with possibility of further digital processing. Sampling time step has to be set equal to the period of modulation ($2T$=2 ms). When writing to the file, it is preferable to use the option Spline Interpolation, which provides better accuracy of the saved data. The file is then processed by an external program, and the results are plotted as a set of dots that visualize the attractor. Figure 8 shows diagrams obtained in such way in the coordinates (x, y), (x, z) and (z, y). Their comparison with Figure 3 clearly demonstrates that we deal here and there actually with one and the same object; the degree of compliance is really good.

IV. REVEALING THE NATURE OF THE ATTRACTOR

At this point it is not so clear that the attractor indeed relates to the type discussed in the Introduction, but really this is the case. First, we note that the unit sphere $x^2 + y^2 + z^2 = 1$ is an invariant set, as seen from the equations, and the attractor belongs to this invariant set. Hence, we can consider a restriction of the dynamical system (2) onto the unit sphere. Now, we represent the attractor on the plane using the stereographic projection. The following variable change is appropriate:

$$X = \frac{z - x}{x + z + \sqrt{2}},\ Y = \frac{y\sqrt{2}}{x + z + \sqrt{2}}. \qquad (4)$$

It corresponds to the projection from the sphere to the plane, with the projection center placed at the point C $(-1/\sqrt{2},\ 0,\ -1/\sqrt{2})$. This point does not belong to the attractor (it is in the "hole"), so the attractor on the plane appears to be located in a bounded domain. In stroboscopic description, the restricted system is governed by a two-dimensional map; one can think of the plane (X, Y) as of the phase space for this map. Figure 9 shows stroboscopic portraits of the attractor on this plane; one obtained from computer integration of equations (2), and the other from processing recorded data of simulation in Multisim.

To reveal that this attractor is of Plykin type discussed in Introduction it is appropriate to turn to graphical representation of the contracting and expanding foliations. To draw the curves defining the contracting foliation we start from a point on the attractor $\mathbf{x}$ and perform integration of the restricted differential equations backward in time for many randomly chosen initial conditions in a small neighborhood of $\mathbf{x}$ over some period $2NT$, where N is some empirically chosen integer, and $2T$ is the switching period. Then, we get a set of images of the starting points, which mark one of the curves determining the contracting foliation. Then the procedure is repeated at

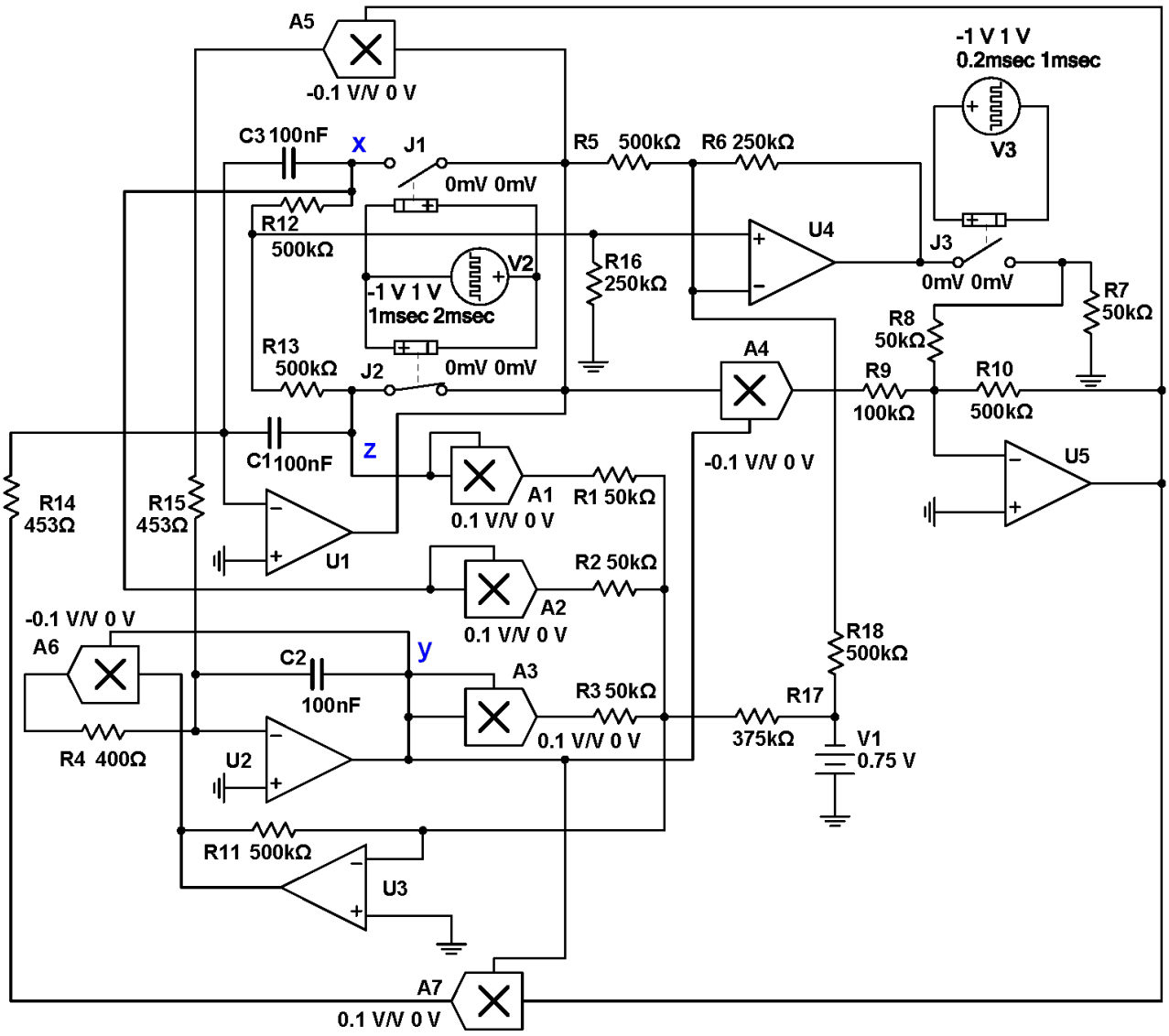

FIG. 4: Circuit diagram of the device. Dynamic variables that characterize the position un the phase space on the unit sphere are voltages on the capacitors C1, C2 and C3, respectively, for z, y, x. Multipliers A1, A2, A3, A7 have positive conversion coefficients for transformation from input to output voltages, and those for A4, A5, A6 are negative; the absolute value of the conversion coefficients is 0.1.

other points on the attractor to recover a representative set of the curves [44]. No efforts needed to visualize the expanding foliation: the respective curves on the plane follow filaments of the attractor. In Fig. 10a the attractor is shown in light gray, and the set of curves obtained form the above procedure is shown in black. Observe that mutual disposition of both families of curves surely exclude tangencies.

Among the curves corresponding to the contracting foliation a particular one is the stable manifold of the saddle fixed point marked with symbol P in Fig. 10b (at the parameters (3) its coordinates are $X{=}0$ and $Y = -3.375817$). Been traced up to sufficient length this curve separates the domain containing the attractor onto seven areas corresponding to elements of the Markov partition. This picture may be compared with the Markov partition [8, 9, 15] for the construction discussed in Section I, see Fig. 10c. Visual comparison of the panels (b) and (c) indicates their obvious topological equivalence. Graf in Fig. 10d represents the rules of transitions between the elements of the partition allowed by the dynamical evolution, which are common for the mathematical example of Plykin-type attractor of Fig. 1 and for attractor of our restricted dynamical system.

Now, let us return to the non-restricted set of equations (2). One test for hyperbolicity of the attractor is based on the computational approach used in [17, 30–32]. The procedure consists in evaluation of vectors of

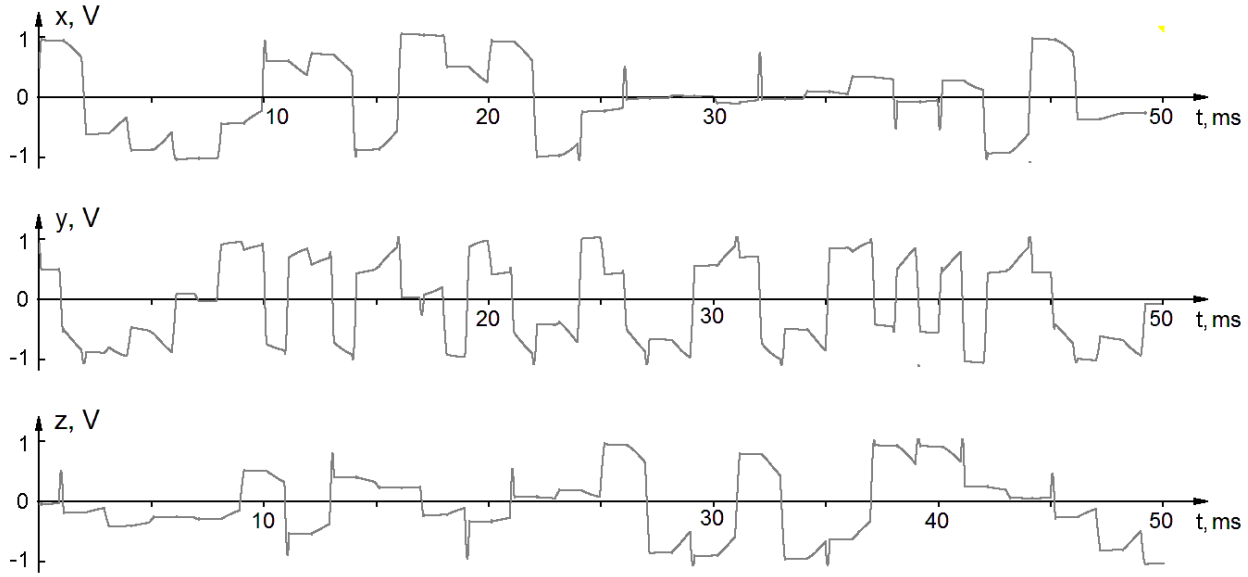

FIG. 5: Time dependences for three variables x, y, z obtained by simulation in Multisim with a use of the multi-channel oscilloscope tool.

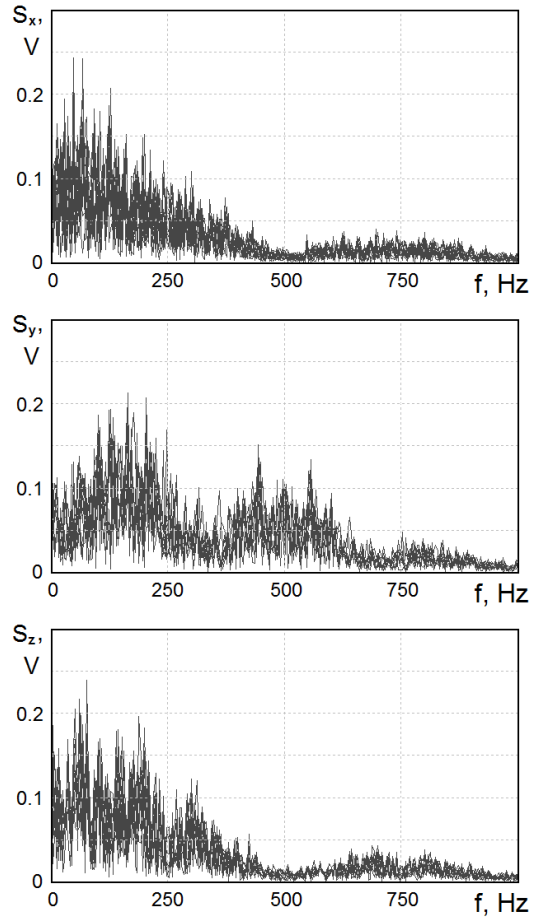

FIG. 6: Spectra of signals corresponding to the variables x, y, z. The resolution frequency is 4 Hz.

small perturbations along a representative orbit on the attractor, with measuring angles between the subspaces of vectors unstable in forward and backward time. If the statistical distribution of the angles is clearly separated from zero the dynamics is detected as hyperbolic. In our case, the forward time unstable subspace is one-dimensional, but in the inverse time we deal with the two-dimensional subspace. The routine starts with generating a long orbit on the attractor from integration of the differential equations (2). Then, the variation equations are solved numerically forward in time with normalization of the resulting vector $\mathbf{a}_n$ after each next period of switching. This vector sampled with the time step $2T$ determines unstable direction at the points of the orbit of the stroboscopic map. Next, along the same trajectory we solve a collection of two replicas of the variation equations in backward time to get vectors $\{\mathbf{b}_n, \mathbf{c}_n\}$, which are orthoganalized by Gram-Schmidt process and normalized at each n. Then, at each n the angle α_n between $\mathbf{a}_n$ and the subspace spanned over the vectors $\{\mathbf{b}_n, \mathbf{c}_n\}$ is evaluated. To do this, we define a vector orthogonal to the two-dimensional subspace, with components determined from the set of two linear algebraic equations $\mathbf{v}_n \cdot \mathbf{b}_n = 0$, $\mathbf{v}_n \cdot \mathbf{c}_n = 0$, then compute an angle between $\mathbf{v}_n$ and $\mathbf{a}_n$ from $\cos\beta_n = |\mathbf{v}_n \cdot \mathbf{a}_n|/|\mathbf{v}_n||\mathbf{a}_n|$, and finally set $\alpha_n = \pi/2 - \beta_n$. Figure 11 shows a histogram for the angles α_n obtained from computations at the indicted parameter values for the system (2). Observe clearly visible separation of the distribution from zero angles. So, the test confirms the hyperbolicity of the attractor.

Additionally, computer verification of the cone criterion [9–11] was undertaken for the attractor of the system (2) at parameters (3). Concrete version of the method is described in the paper [25]. It was applied to a three-

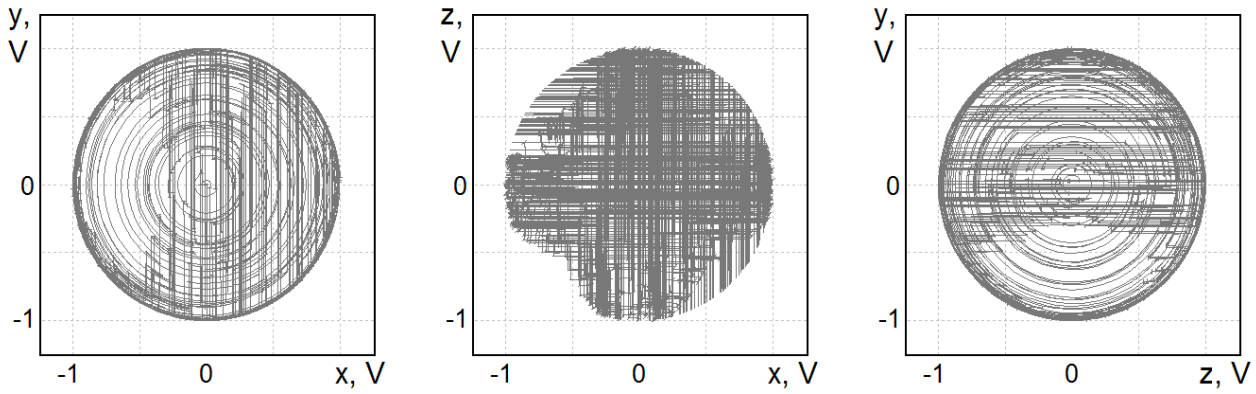

FIG. 7: Portraits of the attractor in three projections on the planes (x, y), (x, z) and (z, y), obtained from the simulation in Multisim by snapshot of the oscilloscope screen.

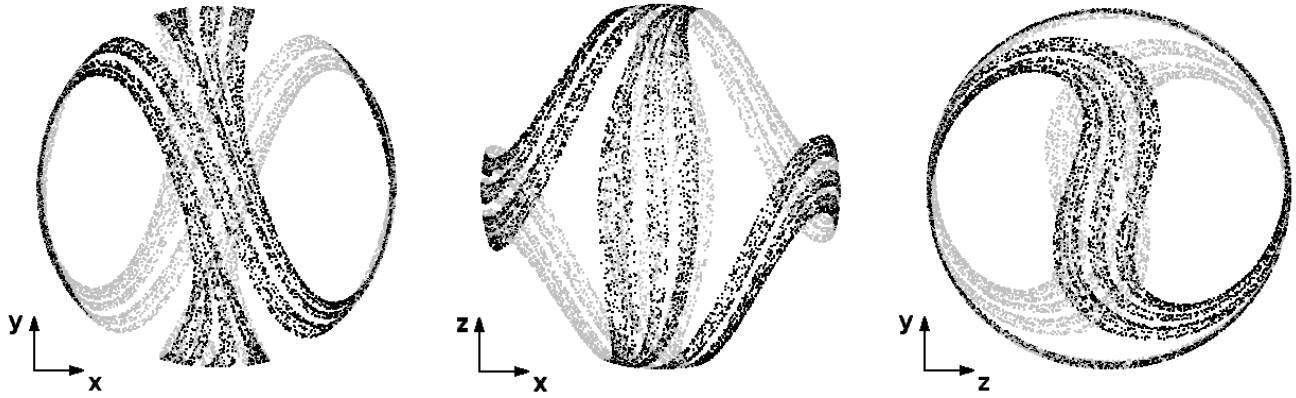

FIG. 8: Portraits of the attractor in the stroboscopic section in projection on the planes (x, y), (x, z) and (z, y), obtained from processing the data of the Multisim simulation saved as time series for x, y, z with sample time step 2 ms.

dimensional map corresponding to two-fold period of switching in the system ($4T$). At a representative set of points on the attractor it was checked (i) existence of the cones of perturbation vectors characterized by expanding and contracting with factor $\Gamma^2 > 1$ for squared norms, and (ii) the invariance of the cones. The last means that for all processed points the image of the expanding cone belongs to interior of the expanding cone defined for the image point, and the pre-image of the contracting cone belongs to interior of the contracting cone defined for the pre-image point. The verification of the criterion was performed for a representative set of points on the attractor obtained from successive iterations of the stroboscopic map. It is believed that the same is true for the entire attractor on the following reason. As the systems is smooth in respect to the variables $\mathbf{x}$, $\mathbf{y}$, $\mathbf{z}$, the objects involved in the procedure of verification of the cone criterion also depend on the state variables in smooth manner because they are determined by the dynamics on finite time interval $4T$. It means that validity of the conditions at some point $\mathbf{x}$ with constant Γ^2 distant from 1 implies that they hold as well in a neighborhood of $\mathbf{x}$ (as wider, as larger the value $\Gamma^2 - 1$ is). Hence, a positive result of the test for a representative set implies validity of the criterion on the attractor, if it is covered completely by the union of the mentioned neighborhoods. Practically, such situation is achieved by increase of the number of points on the attractor subjected to the test, i.e. by increase of the duration of the processed orbit. The computations indicate that the required conditions are valid at least at $\Gamma^2 = 2$ that confirms the uniformly hyperbolic nature of the attractor.

To compute all Lyapunov exponents for the three-dimensional non-autonomous system, joint integration of the differential equations is performed together with a collection of three sets of variation equations for perturbation vectors. After each next period of switching, the Gram–Schmidt process is applied to obtain an orthogonal set of the vectors, and normalization of them to a fixed constant is produced. The Lyapunov exponents are obtained as slopes of the straight lines approximating the accumulating sums of logarithms of the norm ratios for the vectors in dependence on the time of integration [33]. At the particular parameters (3), the Lyapunov ex-

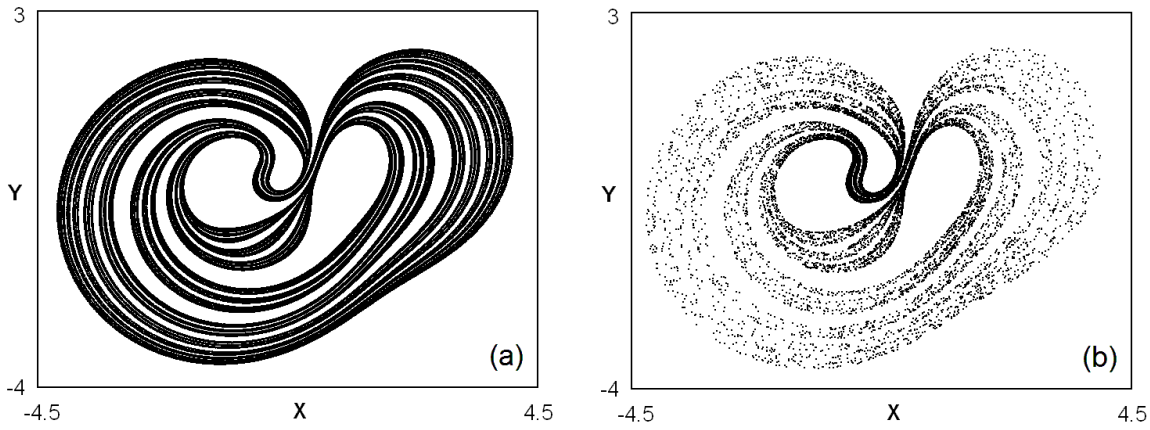

FIG. 9: Stroboscopic portraits of attractor depicted on the plane of the variables (3), one obtained from computer integration of equations (2) (a), and the other from processing recorded data of simulation of the circuit in Multisim (b).

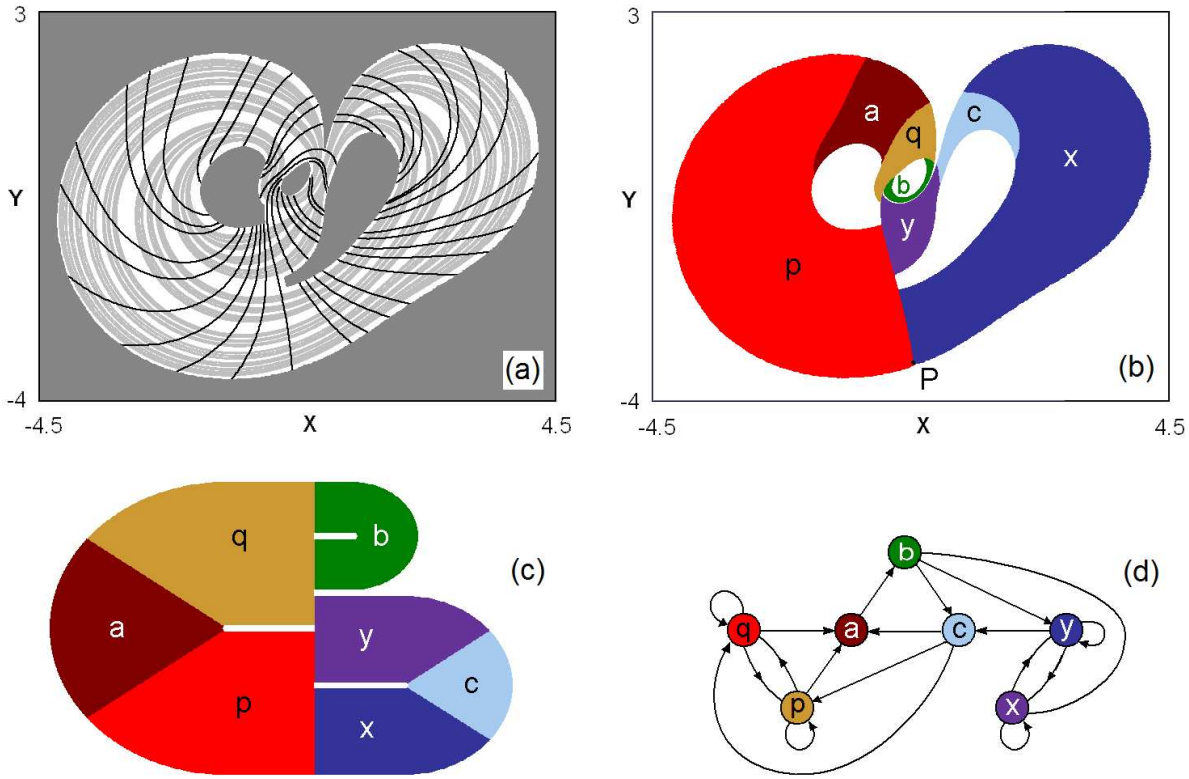

FIG. 10: Visualization of the contracting and expanding foliations (a) and Markov partition of the absorbing domain containing the attractor (b) obtained numerically from the two-dimensional version of equations (2) reduced to the surface of the unit sphere. Markov partition for the Plykin attractor construction corresponding to Fig. 1 (c), and graph illustrating allowed transitions for the both Markov partitions (d).

ponents are $\lambda_1 = 0.0478$, $\lambda_2 = -0.0611$, $\lambda_3 = -0.197$. The largest Lyapunov exponent is positive that indicates chaotic nature of the dynamics. Multiplying by the coefficient $2T$, we get the Lyapunov exponent for the stroboscopic map: $\Lambda_1 = 2T\lambda_1 = 0.956$. This value is close to $\ln(3+\sqrt{5}) \approx 0.9624$, which is the Lyapunov exponent associated with idealized construction of the given Plykin type attractor (see [16]). The second exponent is negative; it is relevant for estimate of the fractal dimension of the attractor from the Kaplan-Yorke formula [34] $D = 1 + \lambda_1/|\lambda_2| \approx 1.78$. The fractional part of the dimension indicates presence of fractal transversal structure. Due to relatively large value of the fractional part, this structure is well pronounced and really visible on the

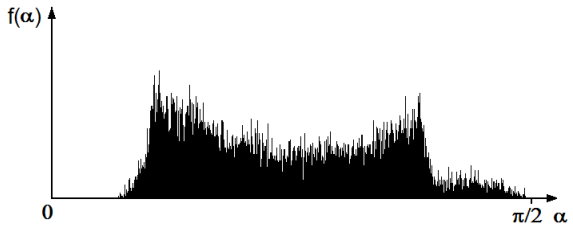

FIG. 11: Histogram for the distributions of angles α between the subspaces of perturbation vectors corresponding to integration in forward and inverse time along representative orbit on the attractor of the system (2) as explained in the text.

stroboscopic portraits of the attractor: the object is built of strips, which contain narrower strips consisting of yet thinner filaments, and so on. The third Lyapunov exponent (negative and the largest in absolute value) is not essential for the structure of the attractor. It describes approach of orbits in the phase space to the invariant sphere, on which the attractor is placed. As one can check, the value of λ_3 is controlled by parameter γ (see (2)), while other Lyapunov exponents do not depend on it notably. It reflects presence of a redundant dimension: the state space of our system is of dimension larger by one in comparison with the minimal needed for occurrence of the Plykin attractor. This is the price for a possibility to arrange this object in the relatively simple setup.

V. CONCLUSION

For the first time, a realistic physical system designed as an electronic circuit us proposed, in which chaotic attractor of Plykin type occurs in the state space of the stroboscopic map governing the dynamics.

The circuit diagram is presented and simulation of the dynamics using the Multisim software package has been performed. For confident interpretation of the attractor as that of Plykin type, the circuit was constructed with the approach used in the analog simulation and computations, aimed to the most adequate reproducing of the underlying differential equations. The equations were constructed in such way that the dynamics in the phase space allows interpretation in terms of continuous transformations on the unite sphere including successive differential rotations around two mutually orthogonal axes.

Verification of the uniform hyperbolicity of the attractor was performed in computations basing on visualization of the contracting foliation (for the restricted version of system on the invariant sphere), on the statistics of the angles between stable and unstable manifolds of the attractor, and on the cone criterion. As the uniform hyperbolicity is confirmed, one can use all conclusions of the hyperbolic theory in respect to the suggested system including chaotic behavior with positive Kolmogorov-Sinai entropy, structural stability, existence of absolutely continuous invariant measure of Sinai-Ruelle-Bowen, existence of finite Markov partition, applicability of the description in terms of symbolic dynamics etc. [2, 4–12].

As the concrete circuit diagram is presented with all indicated element characteristics, it seems not so difficult to implement the scheme as a real electronic device and study it in experiments. Due to the structural stability, its operation is expected to be insensitive in respect to interferences, noises, and at least slight variations of functions and parameters of the constituting elements. In particular, the switching accompanying the operation of the system may be replaced by a smooth transition between the ON and OFF states of the respective elements without destruction of the uniformly hyperbolic chaos (cf. [24, 26]).

Electronic devices with structurally stable hyperbolic chaos similar to that described in the article can find application in systems of chaotic communication [35–37], noise radar [38], as well as for cryptographic schemes [39–41]. One possible application is generation of random numbers [42, 43]. Although the mathematical model (2) in this context should be treated as a Pseudo-Random Number Generator, as a physical device, it should be classified as a True Random Number Generator. Indeed, in the process of dynamical evolution on the attractor is inevitable amplification of noise from the microscopic level to macroscopic quantities by virtue of the inherent chaos of sensitivity to perturbation of the phase trajectories due to presence of a positive Lyapunov exponent. Thus, the physical system under the influence of weak noise selects a trajectory on the attractor really in random way.

Acknowledgments

The work was performed, in part, during a visit of the author to the Group of Statistical Physics and Theory of Chaos in Potsdam University. The research is supported by RFBR-DFG grant 11-02-91334.

[1] A.A. Andronov, A.A. Vitt, S.E. Khaikin, *Theory of oscillators* (Pergamon Press, 1966).
[2] L. Shilnikov, International Journal of Bifurcation and Chaos **7**, 1353 (1997).
[3] M.I. Rabinovich and D.I. Trubetskov, *Oscillations and Waves: In Linear and Nonlinear Systems* (Kluwer Acad. Pub. 1989)
[4] S. Smale, Bull. Amer. Math. Soc. (NS) **73**, 747 (1967)
[5] R.F. Williams, Publications mathématiques de l'I.H.É.S. **43**, 169 (1974)
[6] R.V. Plykin, Math. USSR Sb. **23** (2), 233 (1974).
[7] R.L. Devaney, *An Introduction to Chaotic Dynamical*

Systems (Addison-Wesley, New York, 1989).
[8] J. Guckenheimer and P. Holmes, *Nonlinear Oscillations, Dynamical Systems, and Bifurcations of Vector Fields* (Springer, 2002).
[9] Y.G. Sinai, in: A.V. Gaponov-Grekhov (ed.) Nolinear waves, 192 (Moscow, Nauka 1979) (in Russian).
[10] A. Katok and B. Hasselblatt, *Introduction to the Modern Theory of Dynamical Systems* (Cambridge University Press, 1995).
[11] V. Afraimovich. and S.-B. Hsu, *Lectures on chaotic dynamical systems*, AMS/IP Studies in Advanced Mathematics, **28**, (American Mathematical Society, Providence, RI; International Press, Somerville, MA, 2003).
[12] T.J. Hunt and R.S. MacKay, Nonlinearity **16**, 1499 (2003).
[13] C.A. Morales, Annales de l'Institut Henri Poincaré **13**, 589 (1996).
[14] V. Belykh, I. Belykh, and E. Mosekilde, International Journal of Bifurcation and Chaos **15**, 356 (2005)
[15] T.J. Hunt, *Low Dimensional Dynamics: Bifurcations of Cantori and Realisations of Uniform Hyperbolicity*, PhD Thesis (Univercity of Cambridge, 2000).
[16] J.S. Aidarova, S.P. Kuznetsov, Izvestija VUZov – Prikladnaja Nelineinaja Dinamika **16** (3) 176 (2008). English transl.: http://xxx.lanl.gov/abs/0901.2727.
[17] S.P. Kuznetsov, Phys. Rev. Lett. **95** 144101 (2005).
[18] S.P. Kuznetsov, E.P. Seleznev, JETP **102**, 355 (2006).
[19] S.P. Kuznetsov and A. Pikovsky, Physica D **232**, 87 (2007).
[20] O.B. Isaeva, S.P. Kuznetsov, and E. Mosekilde, Phys. Rev. E **84**, 016228 (2011).
[21] S.P. Kuznetsov, JETP **106**, 380 (2008)
[22] S.P. Kuznetsov, Physics-Uspekhi **54** (2), 119 (2011).
[23] NI Multisim, official website: http://www.ni.com/multisim/
[24] S.P. Kuznetsov, Communications in Nonlinear Science and Numerical Simulation, **14**, 3487 (2009).
[25] S.P. Kuznetsov, CHAOS **19**, 013114 (2009).
[26] S.P. Kuznetsov, Nonlinear Dynamics **5**, 403 (2009) (in Russian).
[27] P. Horowitz and W. Hill, *The Art of Electronics* (Second ed.) (Cambridge University Press, 1989).
[28] L.O. Chua, Scholarpedia **2**(10), 1488 (2007).
[29] P.D. Hiscocks, *Analog Circuit Design* (Syscomp Electronic Design Ltd., 2005-2010). http://syscompdesign.com/AnalogBook.html
[30] Y.-C. Lai, C. Grebogi, J.A. Yorke, I. Kan, Nonlinearity **6**, 779 (1993)
[31] V.S. Anishchenko, A.S. Kopeikin, J. Kurths, T.E. Vadivasova, G.I. Strelkova. Physics Letters A **270**, 301 (2000).
[32] P.V. Kuptsov and S.P. Kuznetsov, Phys. Rev. E **80**, 016205 (2009).
[33] G. Benettin, L. Galgani, A. Giorgilli, J.-M. Strelcyn, Meccanica **15**, 9 (1980).
[34] J.L. Kaplan and J.A. Yorke, in: H.-O. Peitgen and H.-O. Walther (eds.) Functional Differential Equations and Approximations of Fixed Points. Lecture Notes in Mathematics, **730**, 204 (Springer, Berlin, N.Y., 1979).
[35] T. Yang, International Journal of Computational Cognition **2** (2), 81 (2004)
[36] A.S. Dmitriev and A.I. Panas, *Dynamical Chaos: New Information Carriers for Communication Systems* (Moscow, Fizmatlit, 2002) (in Russian).
[37] A.A. Koronovskii, O.I. Moskalenko, A.E. Hramov, Physics – Uspekhi **52**, 1213 (2009)
[38] K.A. Lukin, Telecommunications and Radio-Engineering **16** (12), 8 (2001).
[39] M.S. Baptista, Physics Letters A **240**, 50 (1998).
[40] J.M. Amigó, Intelligent Computing Based on Chaos Studies in Computational Intelligence, Volume 184/2009, 291 (2009)
[41] J.M. Carroll, J. Verhagen, and P.T. Wong, Cryptologia **16** (1) , 52 (1992).
[42] T. Stojanovski and L. Kocarev, IEEE Trans. Circuits and Systems I **48** (3), 281 (2001).
[43] T. Stojanovski, J. Pihl, L. Kocarev, IEEE Trans. Circuits and Systems I **48** (3), 382 (2001).
[44] The accuracy the curves are depicted grows fast with increase of N. Actually, $N = 6$ is enough to get so small errors that they are visually indistinguishable in the plot.